

FRactal Dimension: An Indicator to Characterize the Microstructure of Shale and Tight Gas Sands Considering Distinct Techniques and Phenomena

Mayka Schmitt^{a, b}, Matthias Halisch^b, Celso P. Fernandes^a, Viviane S. S. dos Santos^c,
Andreas Weller^d.

^a Porous Media and Thermophysical Properties Laboratory (LMPT), Mechanical Engineering Department, Federal University of Santa Catarina, 88040900 Florianópolis, SC, Brazil.

^b Leibniz-Institute for Applied Geophysics (LIAG), Dept. 5 - Petrophysics & Borehole Geophysics, 30655 Hannover, Germany.

^c Leopoldo Américo Miguez de Mello Research and Development Center (CENPES-Petrobras), 21941598 Rio de Janeiro, RJ, Brazil

^d Clausthal University of Technology, Institute of Geophysics, 38678 Clausthal, Zellerfeld, Germany.

This paper was prepared for presentation at the International Symposium of the Society of Core Analysts held in Snowmass, Colorado, USA, 21-26 August 2016

ABSTRACT

In this work we focused on the enhanced pore space characterization of shale and tight gas sandstones from Brazilian unconventional reservoirs, using fractal dimension determined by distinct laboratory techniques. The usage of several techniques is essential to properly cover the whole porous scale in shale and tight gas sandstone (TGS) consisting of ultra-fine (nanopore) structures, often associated with clay content and wide pore (fractures) resulting in broad pore sizes distribution. Fractal theory is an effective method that has been applied in geophysics to quantify the complexity of the rocks pore structure. As the rock pore geometry is conventionally divided into the surface geometry and the collective geometry of all the pore space, for the global description of the pore geometry a multifractal approach is presumably required. Routine core analyses, Mercury Intrusion Capillary Pressure (MICP), Nitrogen Gas Adsorption (N₂GA), X-Ray Nano- and Micro-Tomography were applied on two samples, one of each shale and TGS. From the tests statistical quantification of pore geometries and pore size distributions were acquired allowing to determine fractal dimension using, i.a., “fractal FHH” (Frenkel, Halsey, Hill), “Pittman's hyperbola” and 3D box-counting methods. The results show that fractal dimension of shale and TGS reflects their complex pore systems mainly consisting of three defined regions (D₁: macropores, D₂: mesopores and D₃: micropores). Naturally the distinct trends showed by the investigated techniques are expected as each method detects particular pore ranges and textures. In a practical manner both pore structure and surface irregularities play a role in the increases of capacity and rate flow of oil and gas reservoirs.

INTRODUCTION

Fractal analysis has proven to be useful to describe the geometric and structural properties of pores and rough surfaces. According many authors [1] there are two conventional definitions in describing the fractality of porous material: the pore fractal dimension representing the pore distribution irregularity and the surface fractal dimension characterizing the pore surface irregularity. At molecular size and microscopic range, surfaces of most materials including those of natural rocks show irregularities and defects that appear to be self-similar upon variation of resolution. A self-similar object is

characterized by similar structures at different scales. The regularity of self-similar structures can be quantified by the parameter of fractal dimension [2]. The topological dimension of a smooth surface is equal to two, while a rough surface is described by a fractal surface dimension $D_s > 2$. The fractal dimension of a volume distribution can be analyzed in a similar way. A uniform pore-size distribution corresponds to the topological dimension of three, but a variation in the pore-size distribution results in a fractal volume dimension $D_v < 3$. Many studies have shown methods that investigate the relation between capillary pressure and fluid saturation of wetting phase can be used to determine the fractal volume dimension of porous rocks [2]. The capillary pressure P_c in a cylindrical pore with radius r is related to the surface tension σ and contact angle θ between the injected and replaced fluid by:

$$P_c = (2\sigma \cos\theta) / r. \quad (1)$$

Considering the inverse proportionality $P_c \propto 1/r$ and $P_{c \min} = 2\sigma \cos\theta / r_{\max}$ being the capillary pressure related to the largest pore radius (r_{\max}), the cumulative volume fraction V_c in the rock pore structure can be related to the ratio of capillary pressures $P/P_{c \min}$:

$$V_c = (V(< r)) / V = (P_c / P_{c \min})^{(D-3)}. \quad (2)$$

Taking the logarithm to both sides of equation 2 results in:

$$\log V_c = (D - 3) \log P_c - (D - 3) \log P_{c \min}, \quad (3)$$

which describes a linear relation between $\log V_c$ and $\log P_c$. In the case of fractal behavior of the pore volume distribution, the slope (S) of the resulting line in double logarithmic presentation and fractal dimension is $D = 3 - S$.

For analysis of the relative pressures (P/P_o) N_2 adsorption and desorption data, the FHH (Frenkel, Halsey, Hill) equation has been widely used for calculating the fractal dimension and its simple form can be presented as follows [3]:

$$\ln(V/V_o) = K \ln(\ln(P_o/P)) + C, \quad (4)$$

where P is the equilibrium pressure, P_o is N_2 saturation pressure, V is the volume of N_2 adsorbed at each equilibrium pressure and V_o is the volume of N_2 in the monolayer (cm^3/g). K is the power-law exponent, dimensionless and C is the constant of gas adsorption. In the linear relationship between $\ln(V)$ and $\ln(\ln(P_o/P))$ the slope of the plot of $\ln(V)$ versus $\ln(\ln(P_o/P))$ should be equal to K , which can be used to calculate fractal dimension D as $D=3+3K$ in the regime of capillary condensation.

The 3D X-ray Nano- and μ -CT images were reconstructed using a FDK (Feldkamp-Davis-Kress) algorithm [4], data visualization and quantification were performed with Avizo Fire 8.1.0 software [5]. Fractal Dimension (D) representing a reasonable quality index for the reconstructed image is a ratio providing a statistical index of complexity comparing how detail in a fractal pattern changes with the scale at which it is measured. In Avizo software the very popular Box-Counting method [6] is coupled and was used for D measurements.

RESULTS AND DISCUSSION

In this work we used non-wetting (Mercury Intrusion/Extrusion Capillary Pressure) and wetting (Nitrogen Gas Adsorption/Desorption) fluids phase's experiments and 3D image analysis to investigate fractal dimension of rocks from unconventional reservoirs of two basin settings in Brazil. Only the results for one sample of each oil and gas fields are shown and discussed: TGS-59 and Shale-17. Figure 1 depicts the results related to the fluid phases experiments; Figures 2 and 3 show the results obtained from the 3D X-ray Nano and μ -CT image acquisitions; Table 1 gives a summary of the all calculated fractal dimensions.

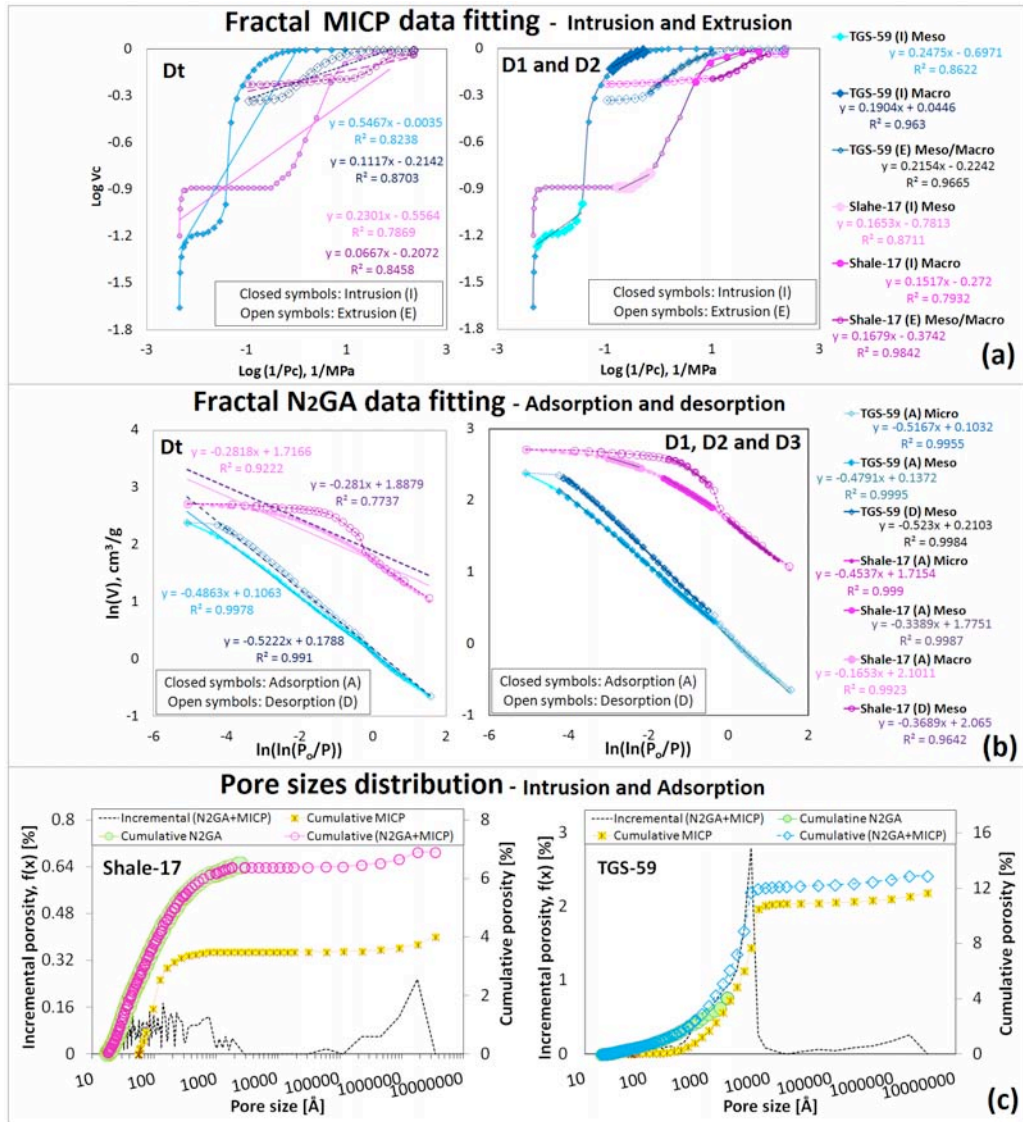


Figure 1. Slopes of the linear equations fitted to the MICP (a) and N₂GA (b) data to calculate: total fractal (Dt), fractal of the macropores (D₁), mesopore (D₂) and micropores (D₃). (c) Range of pore sizes accessed by the two techniques (intrusion and adsorption only).

Table 1. Summary of the fractal dimension values calculated from the distinct pore ranges detected using fluid phases experiment and 3D image analysis.

Samples		Shale-17				TGS-59				
Fluid saturation	Pore size range		Dt	Macro (D ₁)	Meso (D ₂)	Micro (D ₃)	Dt	Macro (D ₁)	Meso (D ₂)	Micro (D ₃)
	MICP	Intrusion	2.77	2.85	2.83		2.45	2.81	2.75	
		Extrusion	2.93	2.83			2.89	2.78		
	N ₂ AD	Adsorption	2.73	2.83	2.66	2.55	2.51		2.52	2.48
Desorption		2.72		2.63	2.55	2.48		2.48	2.48	
X-ray 3D image	Identified pore networks		Org. Matter	Main pores	Ganglia			Main pores	Ganglia	
	μ-CT	VR: 0.75 μm	2.58	2.22	1.95	VR: 1.19 μm	2.43	1.87		
	nano-CT	VR: 0.064 μm	2.65	2.33	1.71	VR: 0.064 μm	2.05	1.37		

VR: Voxel resolution

From the Hg intrusion/extrusion and N₂ adsorption/desorption curves, samples had fractal dimension calculated according to Equation (3) – MICP and Equation (4) – N₂GA data. As shown in Figure 1 (a) and (b), for the overall pore sizes range covered by fittings in the two

techniques a total fractal value (D_t) is predicted; for specific pore range trends fitted separated D_1 , D_2 and D_3 fractal values are calculated. D_1 is, however, more related to the bigger pores and D_3 to the smaller ones; Thus, the relation $D_3 < D_2 < D_1$ is expected with the former referring more to the surface fractal dimension and the two latter describing volume fractal dimension. Figure 1 (c) depicts the pore size ranges covered by N_2GA and MICP individually and in combination [7], elucidating the presence of multimodal distributions and the distinct fractal trends found for both samples. Since the amount of micro- and mesopores ($< 500 \text{ \AA}$) are much higher for Shale-17, a defined D_1 value in the N_2GA data is also showed. The micro and mesopores of Shale-17 are in fact organic hosted pores, associated to the organic matter (OM) observed in this sample, see the darker gray regions on the 2D X-ray CT images (Figure 3). According Loucks et al., 2012 [8], shale pores are classified into: interparticle, intraparticle and organic matter pores. Because OM can be expressed as a percentage share of the mature organic matter (Total Organic Carbon, Wt % TOC) it indicates the potential of a petroleum source rock. OM is also directly related to the organic hosted pores; accordingly, fractal analyses of OM on the 3D images of Shale-17 were performed as well.

Figures 2 and 3 bring the X-ray Nano- and μ -CT results, with the 2D gray-level images and 3D renderings of segmented structures shown on the top graph and, the pore/OM volumes and calculated fractal dimension on the upper part. After performing 3D pore structure segmentation rocks showed very small disconnected pores ganglia plus main pore (MP) networks. As described by Schmitt et al., 2016 [9], the occurrence of pore ganglia obeys the relationship between a detected pore volume (V_p) and its voxel resolution (R_v); the smaller a voxel volume (N_v), the higher its undefined image's grey level and more difficult to identify a clear morphology/geometry. Therefore, a voxel pore volume is characterized as ganglia when the lower cutoff limit is $N_v = V_p / (R_v)^3 \leq 2000$. This explains the very low fractal dimension (approaching surface values) found for ganglia, as they are the smoothest and smaller pore structures identified on the analyzed images. Whereas the structures, total pores (MP+ganglias), MP and OM, showed much higher values. Additionally, fractal values increased for Shale-17 within the higher resolution since many of the smaller pores of this sample were then identified. On the other hand, for TGS-59 the $0.064 \mu\text{m}$ resolution seemed to be more related to the surface fractal dimension and very smooth and around 2 for the main pores identified. All the segmented structures of Shale-17 and TGS-59 showed a trend between the 2D fractal dimension (symbols) and porosity (dot lines) curves, indicating a directly relation. However, the increase in porosity from the 3D analysis does not imply in the rise of fractal dimension value and no correlation was observed for the analyzed samples. Any digitized image with different intensity values on its pixels is conceived as an imperfect cube in which the 3D fractal dimension should be lie in between 2 and 3; Real surfaces and images cannot be true mathematical fractal as they do not exhibit fractal behavior over several scales [10]. As we observed for our samples, fractal dimension will vary depending on the range of pore scales comprised in the acquired image. E.g., $0.064 \mu\text{m}$ resolutions include a sample with axes= $32 \mu\text{m}$; for Shale-17 this size was still enough to achieve fractal characteristics as the values found in the X-ray CT analysis increased from 2.22 ($0.73 \mu\text{m}$) to 2.33, being closer to the value observed in the micro region (D_1) of the N_2GA analysis. Nonetheless, TGS-59 showed a value decreasing from 2.43 ($1.19 \mu\text{m}$) to 2.05, beyond to the value 2.48 found for D_1 . Thus, when determining fractal dimension from 3D images there will have a limited range of pore scales on each of the acquired data set, being the upper limit of this range set by the overall size of the image and lower limit is set by the voxel size.

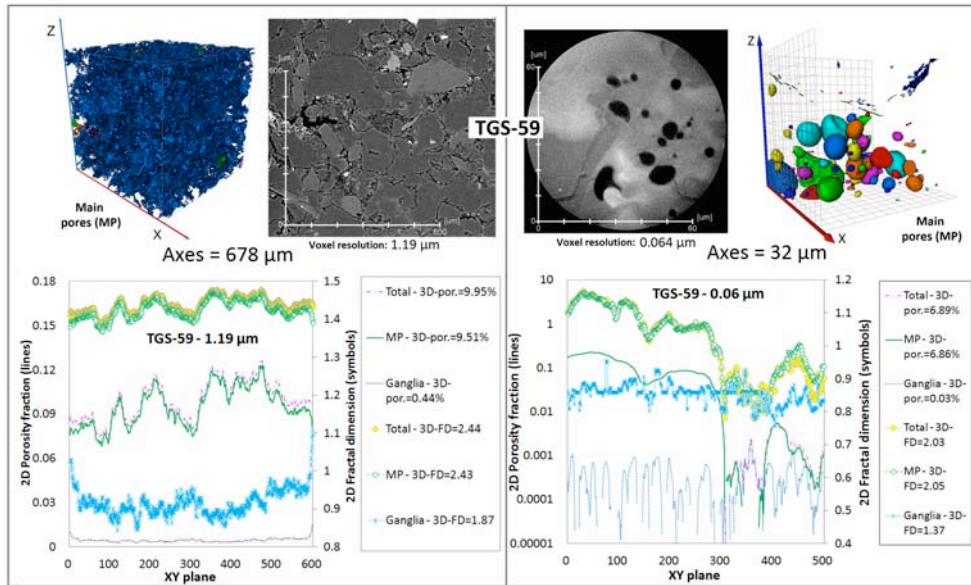


Figure 2. X-ray CT results of TGS-59: 2D gray-level images and 3D segmented pore structures (top part); 2D and 3D results for the fractal dimension and pore volume results (upper graphics).

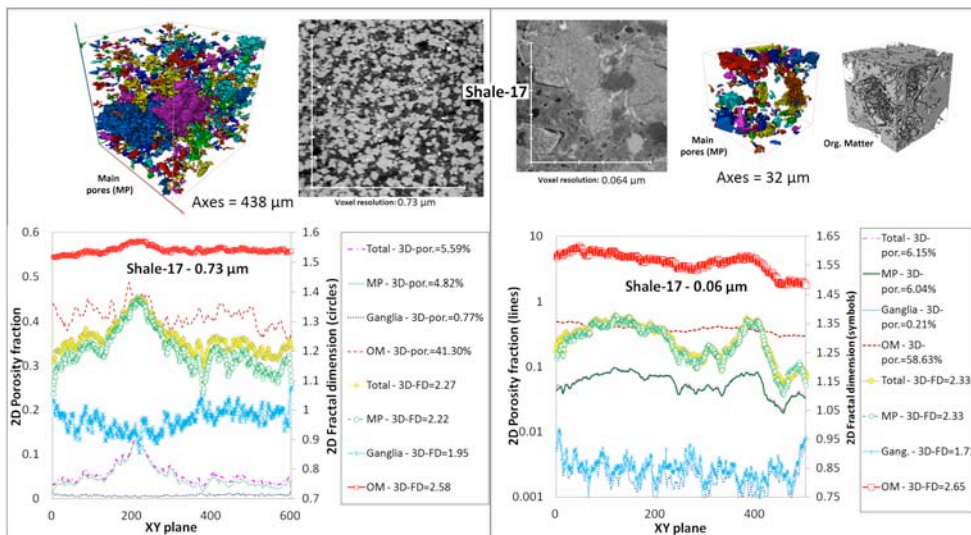


Figure 3. X-ray CT results of Shale-17: 2D gray-level images and 3D segmented pore/OM structures (top part); 2D and 3D results for the fractal dimension and pore/OM volume results (upper graphics).

CONCLUSION AND OUTLOOK

Fractal dimension of pore space in unconventional reservoirs from Brazil was investigated using fluid flow tests and X-ray CT image analyses. Fractals fitted on the drainage and imbibition overall pore size curves showed diverging values higher for MICP than for N₂GA: on Shale-17 values varied between 2.77-2.93 and 2.73-2.72; on TGS-59 from 2.45-2.89 and 2.51-48. This happens because after the imbibition process in MICP a large quantity of the mercury lost continuity and remains in the pore system after reaching atmospheric pressure, resulting in higher fractal dimensions related to the bigger amity pores. From the specific trends revealed on the data curves, macro (D_1) and meso (D_2) pore fractals were calculated from the non-wetting phase experiments and, a micro (D_3) pore fractal was accessed by N₂GA; In both samples $D_3 < D_2 < D_1$ agreeing that D_3 refers to the surface fractal and the two later are more related to the pore volume fractal dimension.

2D and 3D X-Ray Nano- and μ -CT analyses reveals that segmented pore structures seem to carry fractal behaviour; however values are lower compared with those from MICP and N_2 GA curves. Because only a limited range of pores is encompassed by each X-ray CT data set, considerable information from the pore volume structures might be lost, including pore heterogeneities which result in higher fractal values.

Each method was able to reach fractal information from distinct pore ranges and textures. X-ray CT results imply that 3D image fractals are more related to the pore surface geometry as values approached D_3 from N_2 GA. Also, D_2 values calculated from MICP and N_2 GA (for TGS-59 equal 2.75 and 2.52, for Shale-17 equal 2.83 and 2.66) point out the resolution query, the former reports fractal dimension associated to the heterogeneous bigger pore volumes, while the later is more related to the pore surface geometry.

For the ongoing research, other samples of shale and TGS will have the fractal dimension investigated by MICP, N_2 GA and X-Ray Nano- and μ -CT. Thereby, correlations within calculated fractal dimensions and laboratory measurements such as porosity, specific surface area and transient permeability, will be draw to study the role played by pore irregularities in the capacity and increase of flow rate of unconventional reservoirs.

ACKNOWLEDGEMENTS

We would like to thank CNPq, the founding agency of the Ministry of Science, Technology and Innovation of Brazil for granting the research stipend no. 207204/2014-4.

REFERENCES

- [1] Pfeifer, P., Avnir, D., Chemistry in noninteger dimensions between two and three. *Journal of Chemical Physics*, 1983, **79**(7), 3369-3558.
- [2] Zhang, Z., Weller, A. Fractal dimension of pore-space geometry of an Eocene sandstone formation. *Geophysics*, 2014, **79**, 6, 377-387.
- [3] Liang, L., Xiong, J., Liu, X. An investigation of the fractal characteristics of the Upper Ordovician Wufeng Formation shale using nitrogen adsorption analysis. *Journal of Natural Gas Science and Engineering*, 2015, **27**(2), 402-409.
- [4] Feldkamp, L.A., Davis, L.C., Kress, J.W. Practical cone beam algorithm. *Journal of the Optical Society of America A*, 1984, 1(6), 612-619.
- [5] Avizo Fire 8.1.0: 1995–2014©, FEI, SAS – Visualization Sciences Group, Hillsboro, USA, www.fei.com (last access: 20 June 2016), 2014.
- [6] Liebovitch, L.S., Toth, T. A fast algorithm to determine fractal dimensions by box counting. *Physics Letters A*, 1989, **141**, 386-390.
- [7] Schmitt, M., Fernandes, C.P., Da Cunha Neto, J.A.B., Wolf, F.G., Dos Santo, V.S.S. Characterization of pore systems in seal rocks using Nitrogen Gas Adsorption combined with Mercury Injection Capillary Pressure techniques. *Marine and Petroleum Geology*, 2013, **39**(1), 138-149.
- [8] Louck, R.G., Reed, R.M., Ruppel, S.C., Hammes, U. Spectrum of pore types and networks in mudrocks and a descriptive classification for matrix-related mudrock pores. *AAPG Bulletin*, 2012, 96, 1071-1098.
- [9] Schmitt, M., Halisch, M., Müller, C., Fernandes, C.P. Classification and quantification of pore shapes in sandstone reservoir rocks with 3-D X-ray micro-computed tomography. *Solid Earth*, 2016, **7**, 285-300.
- [10] Sarkar, S., Pandey, D., Rathore, K., Munshi, P. Estimation of Moisture Content in Edible Pulses by the Application of Computerized Tomography. *NDE2015, Hyderabad*, November 26-28, 2015, 6 pages.